



Contents list available at CBIORE journal website

International Journal of Renewable Energy Development

Journal homepage: <https://ijred.cbiorc.id>



Research Article

Parametric and characteristic evaluation of microwave-assisted pyrolysis for the generation of biochar from *Dodonaea viscosa* branches

Safa Waleed Shakir^{a,b*} and Atheer Mohammad Al-Yaqobi^b

^aDepartment of Chemical Engineering, College of Engineering, University of Tikrit, Iraq

^bDepartment of Chemical Engineering, College of Engineering, University of Baghdad, Iraq

Abstract. This investigation focused on assessing the feasibility of biochar production through microwave pyrolysis of *Dodonaea viscosa* branches. It considered the role of various important parameters, such as the power levels, biomass particle sizes, and the duration of pyrolysis, on both the yield and the quality of the obtained biochar. The assessment was conducted within a 25-minute pyrolysis time frame. The study also looked at how the yield of biochar changed over time. The results showed that the maximum biochar yield was obtained under conditions where the biomass particles were large (2–2.5 mm) and the power levels low (130 W). However, the yield was reduced when the biomass particles (0.5–1 mm) under higher power (650 W) were used. It was found that the yield of particles 2–2.5 mm dropped from 82% for 5 minutes at 130 W to 49.8% for 25 minutes. Further research has examined the dynamics of power variation on biochar characteristics. Several types of analysis were used to find out the surface area and pore volume. These included energy dispersive X-ray spectrometry (EDX), scanning electron microscopy (SEM), X-ray diffraction (XRD), Fourier transform infrared spectrophotometry (FTIR), and Brunauer-Emmett-Teller (BET) analysis. The EDX analysis showed an increment in carbon to 89.7%, accompanied by a decrease in oxygen percentage to 4.9% under higher power. The SEM scan showed a tremendous improvement in pore formation corresponding to higher power. The XRD test showed that biochar went from being crystalline to being amorphous when compared to the native *Dodonaea viscosa* branch. At 520 W for 25 minutes, the surface area increased from 3.034 m²/g to 21.634 m²/g, while the pore diameter increased from 2.653 nm to 13.215 nm, showing an improvement in pore density. The results realized that the biochar obtained from microwave pyrolysis of *Dodonaea viscosa* branches has certain characteristics that make it useful for several purposes, like electricity production, water and gas treatment, soil improvement, and carbon dioxide gas reduction.

Keywords: biomass, *Dodonaea v.* branch, microwave-assistant pyrolysis, biochar, characterization



@ The author(s). Published by CBIORE. This is an open access article under the CC BY-SA license (<http://creativecommons.org/licenses/by-sa/4.0/>).

Received: 8th March 2025; Revised: 17th May 2025; Accepted: 31st May 2025; Available online: 14th June 2025

1. Introduction

Recently, pyrolysis has become a more popular way to change biomass. As Majeed *et al.* (2017) and Balaguer *et al.* (2023) stated, biochar is a carbon-rich material that can be used to dispose of agricultural solid waste sustainably and efficiently. A process called pyrolysis (Chen *et al.* 2024) usually turns biomass into biochar. It involves heating organic materials in an oxygen-free environment. The porous biochar has become a relevant field of study due to its high degree of porosity, large surface area, numerous functional groups, and significant conductive properties. Furthermore, the biochar made from agricultural waste has a lot of potential. It can be used to fix soil problems (Song *et al.* 2022), remove heavy metals (Huang *et al.* 2019), clean things up (Siipola *et al.* 2020; Xie *et al.* 2021; Shakir *et al.* 2024), and in other ways in the electrochemical and catalyst fields (Gholizadeh *et al.* 2021).

Additionally, the adopted technology of the pyrolysis process and the nature of the feedstock are strongly empowering the characterizations of biochar (Uday *et al.* 2022; Khawkomol *et al.* 2021). Many researchers have investigated the factors that influenced the surface chemistry and physical

properties of the char formed during the pyrolysis process. These factors included temperature, pyrolysis period, rate of heating, and particle size of the biomass. The results indicated that the level of pyrolysis temperature is crucial for changing the biochar's properties and how it is distributed (Abd *et al.*, 2023; Cheng *et al.*, 2021). Traditionally, pyrolysis processes use a furnace in a tube or muffle with electric heating. The heat is moved to the biomass through convection, radiation, and conduction, and the biomass particles get hotter from the outside to the inside (Zhang *et al.*, 2015a; Mahmood *et al.*, 2024; Mahmood *et al.*, 2021).

Nevertheless, another technique for pyrolysis has been getting more attention due to its advantages compared with the traditional method. The microwave pyrolysis process provides the biomass with internal heating and uniform distribution of temperature. Furthermore, the conversion efficiency using the microwave pyrolysis technique was high (Zhang *et al.* 2015a, Abd 2023). This unique heating principle causes microwave radiation to collide with polar molecules inside the material, converting electromagnetic energy to internal energy and raising the material's temperature. Thus, the material is heated quickly and evenly (Abbas *et al.* 2016; Wang *et al.* 2020a).

* Corresponding author
Email: eng.safawaleed@tu.edu.iq (S.W.Shakir)

Furthermore, microwave pyrolysis is one of the most crucial ways to activate and modify the biochar surface. This approach allows for production of various types of biochar by adjusting the conditions of microwave pyrolysis and selecting the biochar with the desired properties. Studies on biochar's properties show that it has a relatively high surface area because it is porous and contains many minerals (Ahmed *et al.* 2019; Hou *et al.* 2021). Abd *et al.* (2023), who looked at how to break down Albizia branches using high heat, showed that low power levels led to more biochar production, with a 70% yield when 300 W was used for 5 minutes. Furthermore, Qiu *et al.* (2023) investigated microwave-assisted pyrolysis to produce biochar from peanut shells. The yields ranged from 30.04 to 43.38 wt. % at the power level range (400-600 W) for 1-3 hr.

On the other hand, oxygen's chemisorption onto the carbon surface greatly influences most biochar characteristics. The main causes of these functional groups are the selection of the starting material, the heat treatment technique, and the subsequent chemical treatment. Previous studies have shown that these groups, which are directly bound to carbon, play a crucial role in improving the diverse catalytic and physicochemical properties of the material. Because these materials have many functional groups and a basic structure, studying and changing these groups is a good way to make them better or more useful. Zhu *et al.* (2015) studied microwave pyrolysis in corn stoves with a focus on understanding the effect of three major pyrolysis factors on surface properties and the production of biochar. In comparison to corn stover biochar formed using conventional pyrolysis, the biochar produced by microwave pyrolysis at 600°C had a maximum surface area of 45 m²/g.

Consequently, pyrolysis with microwave assistance is a possible technique for producing biochar with a high degree of porosity. Modifying and characterizing the functional groups on the surface of biochar is a promising approach to enhance or expand its catalytic application. While numerous studies have been conducted on the microwave-assisted pyrolysis (MAP) of conventional biomass feedstocks, such as wood, corn straw, and crop waste, there is still a significant body of incomplete knowledge on the use of underutilized feedstocks, such as *Dodonaea viscosa*. Although *Dodonaea viscosa* is cultivated in Iraq not only for its ornamental purposes but also for its tolerance to arid conditions, demonstrating significant success in combating desertification and stabilizing eroded soils, its biomass byproducts are typically underutilized (Sandhya *et al.*, 2009; Hamadi *et al.*, 2017).

While MAP technology in general has typically been applied to conventional biomass feedstocks like wood, maize straw, and

crop residue, the present study is the first to utilise *Dodonaea viscosa*. shoots, a considerably underutilised raw feedstock material. *Dodonaea viscosa* is unusual in that it grows in abundance in arid and semi-arid environments, including in Iraq, where it's prized for its hardness and environmental value, such as desertification prevention (Sandhya *et al.*, 2009; Hamadi *et al.*, 2017; Liu *et al.*, 2022; Castañeda-Espinoza *et al.*, 2023). By turning the previously unused plant material into biochar, this work helps with waste management and uses a type of biomass that has unique chemical and physical traits, which could lead to new biochar features (Kumar *et al.*, 2022; Castañeda-Espinoza *et al.*, 2023; Ke *et al.*, 2024). Additionally, the work clearly explains how to use *Dodonaea viscosa* including the microwave power, particle size, and heating time details that haven't been reported in earlier studies of this type of plant material. The careful study of these factors provides valuable information on how *Dodonaea viscosa* behaves and reacts when it was heated during pyrolysis. Also, the study used several advanced techniques, such as scanning electron microscopy, EDX, XRD, FTIR, and BET, to look at the surface structure, chemical makeup, crystal structure, and pore size of the created biochar material. These analyses play a central role in evaluating the catalytic potential of the resulting biochar material. Additionally, the converting and optimising of the surface characteristics of the biochar composed of *D. viscosa* could be a prospective player in catalytic and environmental applications (Liu *et al.*, 2022; Castañeda-Espinoza *et al.*, 2023).

2. Experimental

2.1 Processing of biomass

Dodonaea viscosa is abundant in many regions of Iraq. The branches were collected from Tikrit University/College of Engineering. After trimming the *Dodonaea viscosa* tree, the agricultural waste branches are collected, washed, and oven-dried at 60°C for 24 hr., and the branches are weighed before and after drying to track the moisture loss. Thereafter pulverized, ground, mesh-screened, and kept in a sealed container.

2.2 The pyrolysis experimental procedure

A microwave oven with a maximum power of 1300 W (MCR-3 manufactured by ZZKD China) was used for pyrolysis with five power percentages (10, 20, 30, 40, and 50%). The oven is equipped with a Pyrex three-neck glass reactor used as a pyrolysis reactor. The experiments were conducted at various particle sizes (0.5-2.5mm) and pyrolysis durations (5-25 min.).

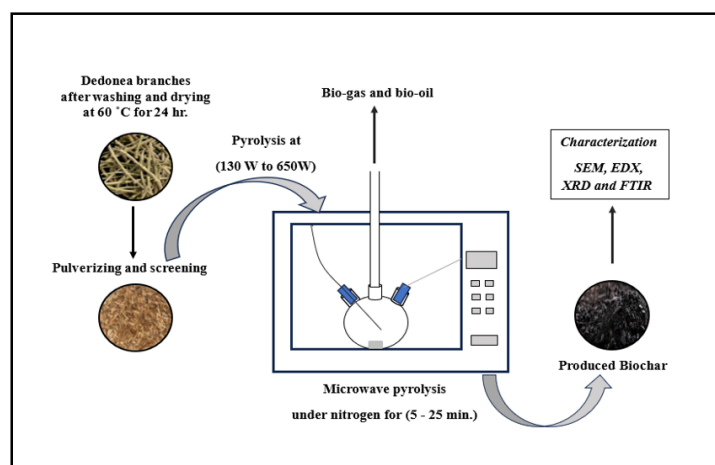


Fig 1. Schematic diagram of microwave pyrolysis process

40 g of processed biomass was replaced in the reactor, which connected with an inlet pipe to introduce inert N₂ gas (98% purity) and another mouth with a thermometer to measure the temperature during decomposition, and the last one for exhaust. of volatiles (pyrolysis product). Figure 1 shows the pyrolysis setup used to conduct the experiments. The outlet of the reactor is directed outside the oven to dispose of pyrolysis gases. The biochar production is calculated according to the equation (1):

$$Y_{\text{biochar}} = \frac{W_{\text{biochar}}}{W_{\text{biomass}}} \times 100 \% \quad (1)$$

Where Y_{biochar} represents the yield of biochar, W_{biochar} the weight of the sample after pyrolysis (g), and the W_{biomass} weight of the biomass sample (g).

2.3. Characterization of Biochar

The characterization of *Dodonaea viscosa* branches produced at different microwave energies was analysed. The Scanning Electron Microscope (SEM), manufactured by MIRA III-Tescan/Czech, provides the energy dispersive X-ray (EDX) and scanning electron microscope (SEM) tests. Magnifications of 25×, 1000×, and 4000× were used to capture the images. The atomic and component weight percentages were ascertained using the same SEM-EDX apparatus. To determine the elemental compositions, the biomass samples were tested without additional treatment. The X-ray diffraction (XRD) spectra were distinguished by X-ray diffraction (PW1730 manufactured by Philips-Netherlands) with a scan range of 2θ from 10 to 90°. The BET test was conducted by the Prep 060 and Gemini BET machines to measure the surface area and specific size of the biochar, and the measurements were made, and the required functions or factors were extracted using several methods, which are the BET method, Langmuir method, t-method, and BHJ method. The Fourier transform infrared has been used to examine the biochar samples' functional groups. FT-IR Spectrometer, Spectrum, Perkin Elmer, and Spectroscopy 2). Their spectra had been obtained with a phase dimension of 1/cm and a scanning rate of 8 within the wavenumber range of 500–4000 1/cm.

3. Result and discussion

3.1 Impact of power level

The impact of microwave energy on biomass decomposition is an important topic that has been studied by many researchers, as studies have indicated that the energy used has significant effects on the quantity and quality of the products resulting from this process is known as the decomposition process. Figure 2 shows the effect of energy levels on the quality and quantity of the pyrolysis process. Changing the power level from 130 W to 650 W decreases the charge remarkably to 10.3%. The reaction temperature goes up as the microwave power goes up, which makes it easier for biomass, complex structures in raw materials, and volatile components to be released. The maximal biochar yield obtained was 49% at 130 W for a particle size of 2.5 mm. The weight loss associated with the breakdown of the biomass remaining lignin and specific minerals affects the amount of the produced biochar (Conte *et al.* 2021). The removal of highly volatile substances from lignin usually accounts for this, as lignin decomposes primarily at high power levels. Increasing the power level resulted in a decrease in the amount of biochar produced. The biochar value turned to a

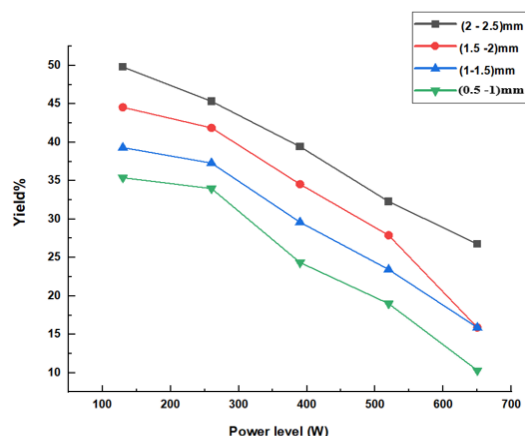


Fig 2. The microwave power level impact on the biochar yield pyrolyzed for 25 min. at different particle size

lower value when the energy level increased to a higher level, which led to an increase in temperature through a series of isomerization, depolymerization, and carbonization reactions that led to the formation of more stable structures (Hassan *et al.*, 2020). When the energy level was raised above 130 W, the decomposition of lignin in the biomass occurred, producing volatile compounds (such as carbon dioxide, carbon monoxide, and water). This degradation was due to aromatic rearrangement reactions, which broke the C-C bond in the biochar (Gao *et al.*, 2020). Furthermore, the breakdown of hemicellulose in biomass is linked to the breakdown of lignin, which is thought to move on to oxidation because of the way it is arranged and its low molecular weight (Huang *et al.*, 2021; Siva *et al.*, 2021). Selective heating of biomass components is perhaps the most significant among these effects because increasing the heating rate increases the rate of evaporating water and the decomposition rate of hemicellulose, cellulose, and lignin. Also, the high-power levels bring about enhanced pore formation, carbonization, and enhanced biochar surface area. However, excessive power, though, can cause non-homogeneous heating, which would generate thermal gradients, low-quality pyrolyzed material, or localized overheating and hence reduce the quality of the biochar. The power of energy also influences the carbon-to-oxygen ratio by enhancing volatile gas and tar formation, hence changing the properties of biochar like surface chemistry and porosity. Such understanding allows process parameters like power level, particle size, and pyrolysis time to be optimized, thereby ensuring the optimized production of biochar for particular applications, e.g., soil amendment, water treatment, and carbon sequestration. A new technology for sustainable production of biochar, microwave-assisted pyrolysis, is a more energy-efficient and controlled biomass decomposition process in general. Also, to evaluate the performance of *Dodonaea viscosa* with another feedstock, Table 1 lists the different feedstocks of microwave pyrolysis and their corresponding product yields influenced by microwave power. At 130 W, *Dodonaea viscosa* exhibits significant variability in the yield range of 49-27% bio-oil and 49-27% char, suggesting it is a non-steady thermal process at low power. Heating wood biomass to 800 W produces a mixed product comprising about 50-60% bio-oil, 30-40% char, and 10-20% gas. Such a mix is usual for lignocellulosic feedstocks. Lignocellulosic feedstocks typically have a balanced product distribution of 50-60% bio-oil, 30-40% char, and 10-20% gas. Plastic waste, at 1000 W, produces 45-55% bio-oil, 20-25%

Table 1
The summary of microwave pyrolysis of various feedstock

Feedstock	Microwave Power Level (W)	Yield (wt.%)	Product Distribution	Reference
Wood (biomass)	800	40	Char: 40%, Bio-oil: 50%, Gas: 10%	(Guo, <i>et al.</i> 2023)
Plastic waste	1000	25	Char: 25%, Bio-oil: 50%, Gas: 25%	(Yang <i>et al.</i> , 2023)
Oil Palm Empty Fruit Bunch (EFB)	300	35	Char: 35%, Bio-oil: 20%, Gas:45 %	(Paikamnam <i>et al.</i> , 2021).
Algal (Nannochloropsis)	1000	9.3	Char: 9.3%, Bio-oil: 50%, Gas: 40.5%	(Lu <i>et al.</i> , 2023)
Pine Sawdust	600	15.0	Char: 15%, Bio-oil: 49.0%, Gas: 36.0%	(Khelfa <i>et al.</i> , 2020)
Albizia	300 W	70	Char: 70%, Bio-oil: 26.0%, Gas: 4.0%	(Abd <i>et al.</i> , 2023)
Albizia	700 W	46	Char: 46%, Bio-oil: 28.0%, Gas: 31.0%	(Abd <i>et al.</i> , 2023)
Dedonea	130	49	Char: 49%, Volatile: 41%,	[current study]

char, and 20–25% petrol, suggesting it is a very promising candidate for liquid fuel production given the simple breakdown of polymers at high power levels. At 300 W, oil palm empty fruit bunch (EFB) produces 32-35% char and 20-26% bio-oil, with significant char generation owing to its high lignin concentration.

Studies have also shown that operation with *Nannochloropsis*, under power of below 1,000 watts, produces similar amounts of gas and biooil, 40.5% each, and little char (9.3%). Being high in lipid percentage, it is a suitable material for the use of biofuel production (Jamilatun *et al.*, 2019; Hadiyanto *et al.* 2012). Pine sawdust, under power of below 600 watts, produces 49% biooil, 15% char, and 36% gas, showing its cellulose structure and intermediate pyrolysis system. While the yield of char from Albizia pyrolysis is high at 300 watts (70%), the biooil yield (26%) and gas yield (4%) are low, indicating incomplete pyrolysis. At 700 watts, char yield is reduced to 46%, biooil yield is marginally increased to 28%, and gas yield is increased significantly to 31%, indicating more thermal cracking and volatiles release. As the power goes up, gas production increases, which indicates more efficiency in secondary reactions and syngas production. Decline in power makes char production higher, beneficial for biochar, while power increase is beneficial for pyrolysis oil and biogas production, hence Albizia was best for producing biofuel. The findings show that microwave power increases pyrolysis, with increased power levels enhancing decomposition efficiency and volatile product formation. The differences in product distribution from these feedstocks demonstrate the effect of adjusting different microwave powers to maximize production: the more power used, the higher oil and biogas yield, while reduced power increases char yield, especially for lignocellulosic feedstocks.

3.2 Impact of particle size

Particle size is another important factor that affects the value and yield of a product. All pyrolysis tests used the same amount of weight, despite the variation in particle sizes. Forty grammes of treated *Dodonaea viscosa* branches were used with particle sizes ranging from 0.5 mm to 1 mm, 1-1.5 mm, 1.5 mm to 2 mm, and 2-2.5 mm. The power levels employed were 130 W, 260 W, 390 W, and 650 W. The data were shown over a 25-minute pyrolysis period. Figure 3 shows different particle sizes during 25 min of pyrolysis at various power levels. Figure 3 shows unambiguously that the greatest biochar output came from using large particle sizes at low power levels. The 130 W output, for instance, was 49%. A 10% drop in biochar output came from using a tiny particle size at a 650 W power level. The

results indicated that the yield of biochar drops by increasing microwave power. The yield fell from 49% to 27% when the power level increased from 130 to 650 W at a particle size of 2–2.5 mm. Conversely, when using a smaller particle size (1 mm) at 130 W, the char production percentage dropped to 35.4%. The pyrolysis of small particles causes overheating, which causes secondary reactions like carbonisation, cracking, and polymerisation. On the other hand, bigger particle sizes could produce more biochar because of limited heat transfer and lower heating rates, which cause partial pyrolysis. Larger particles might also require more time to pyrolyze, which raises the likelihood of char creation and secondary reactions (Suresh *et al.* 2021; Abd *et al.* 2022). The microwave energy might not penetrate deeply enough as particle size grows, therefore prolonging the core's coolness. As a result, uneven biochar characteristics across the particles or incomplete pyrolysis can happen; the outer layers show more carbonization and porosity, while the inner areas keep more of original structure. To address this challenge, we select the 2.5 mm particle as the largest size capable of effective pyrolysis.

3.3 Impact of time

The pyrolysis period influences the amount and nature of products obtained from biomass conversion using microwave pyrolysis. A time range of 5-25 min. was used to investigate how the pyrolysis period affected biochar production at various power levels and particle sizes throughout the pyrolysis duration, reaching its maximum percentage at 25 minutes.

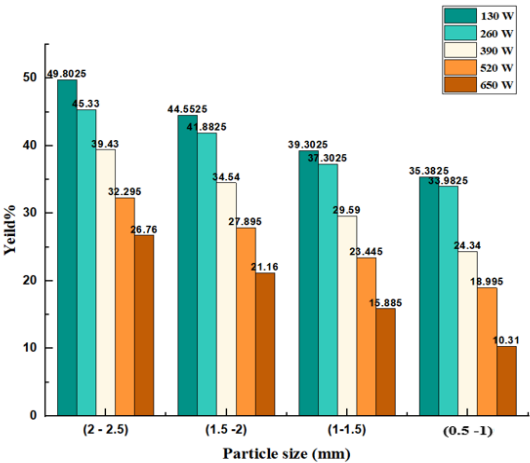


Fig 3. The effect of particle size on the biochar yield at different power level pyrolyzed for 25 min.

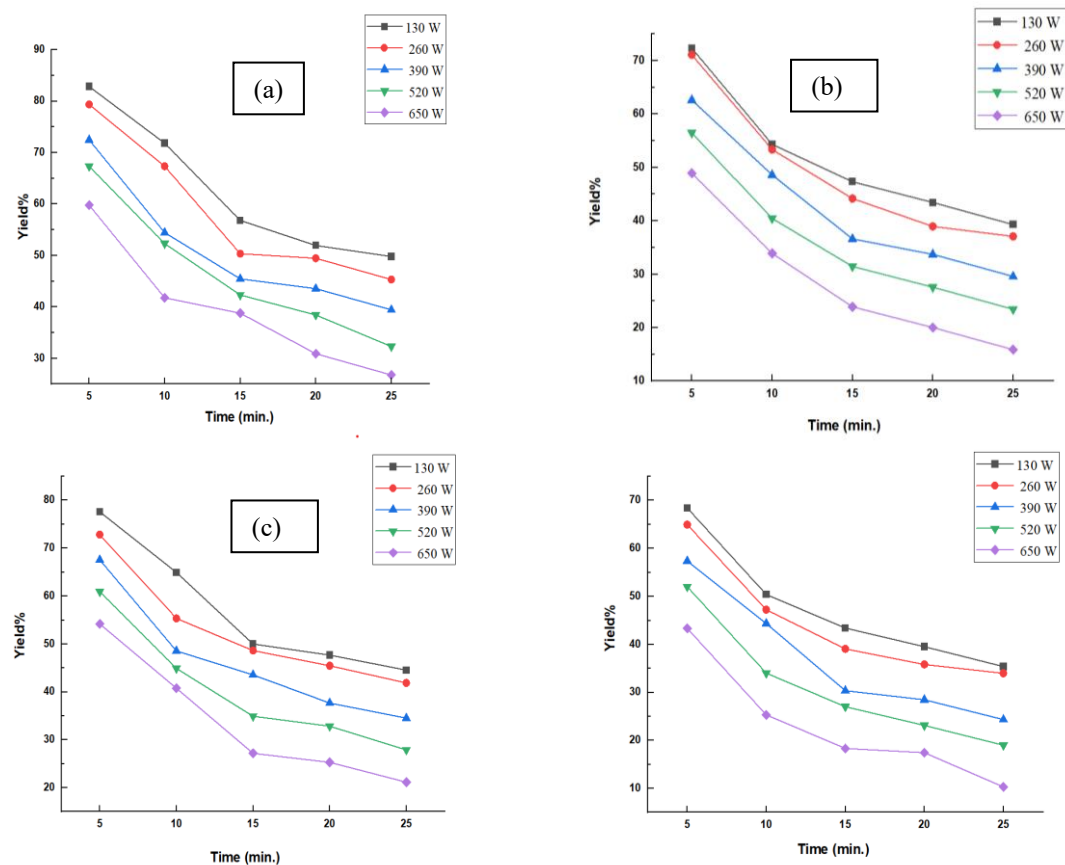


Fig 4. the influence of pyrolysis period on the biochar yield at different power level at A) particle size of (2-2.5 mm) B) particle size of (1.5-2 mm) C) particle size of (1-1.5 mm) D) particle size of (0.5-1 mm)

Figure 4 shows that biomass yield ranged from 82% at 130 W for 5 minutes to 49.8% after 25 minutes at a particle size of 2-2.5 mm. Furthermore, due to rising temperatures, the yield decreased from 49.8% to 45% as the power increased to 260 W at the same particle size. While, as power levels increased beyond what was permitted, the biochar yield decreased significantly. Over time, the biochar yield decreased at all

permitted energy levels. On the other hand, a shorter pyrolysis time may result in incomplete pyrolysis, lowering the volatile yield while increasing the biochar percentage. Also, longer pyrolysis times may result in volatile component release, cracking, polymerization, and condensation reactions, which The process formed undesirable byproducts, such as tar and coke, which negatively influence both process efficiency and

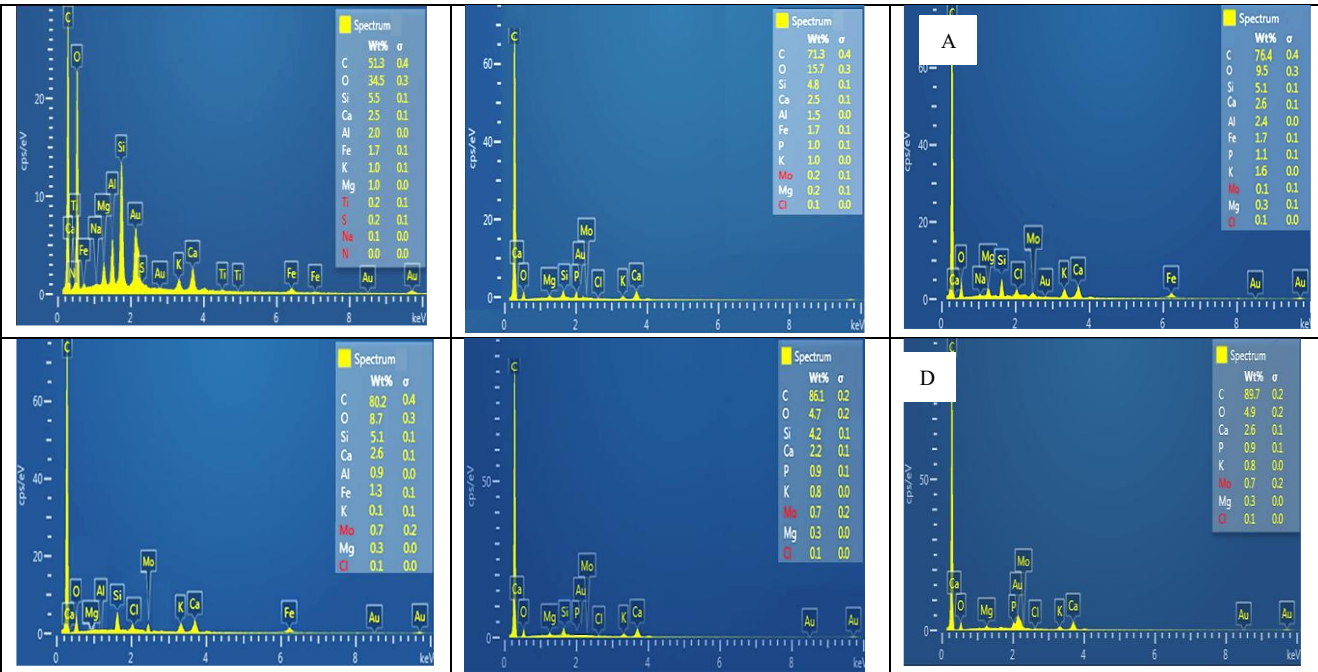


Fig 5. EDX of biochar and *Dedonea* branches at various power level A) *Dedonea* branches B)130 W C)260W D)390W E) 520W F)650W

Table 2
Element analysis of biochar obtained from different power level pyrolyzed for 20 min at different microwave power level.

Element	Dedonea	130 W	260W	390 W	520W	650W
C	51.3	71.3	76.39	80.2	86.1	89.7
N	0.000	0.000	0.000	0.000	0.000	0.000
O	34.5	15.75	9.55	8.7	4.7	4.9
Na	0.06	0.06	0.00	0.00	0.00	0.00
Mg	0.96	0.2	0.3	0.3	0.3	0.28
Al	2.01	1.5	1.4	0.9	0.00	0.000
Si	5.5	4.8	5.1	5.1	4.2	0.00
S	0.24	0.00	0.00	0.00	0.00	0.00
K	1.01	1	1.6	0.1	0.8	0.82
Ca	2.5	2.5	2.6	2.6	2.2	2.6
Ti	0.25	0.00	0.00	0.00	0.00	0.00
Fe	1.67	1.67	1.7	1.3	0.00	0.00
P	0.00	1.0	1.1	0.00	0.9	0.9
Cl	0.00	0.1	0.1	0.1	0.1	0.1
Mo	0.00	0.2	0.1	0.7	0.7	0.7
Over-all	100.00	100.00	100.00	100.00	100.00	100.00

product quality (Abd *et al.*, 2023). Choosing the pyrolysis period improves the process's selectivity for the preferred products. Microwave pyrolysis of *Dodonaea viscosa* branches resulted in a maximum biochar yield of 49% at 130 W and particle sizes of 2.0 to 2.5 mm after 25 minutes. Abd *et al.* (2023) investigated the microwave pyrolysis of Albizia branch. The study found that shorter pyrolysis time and higher applied power, resulted in better biochar production, with a char yield of 70% when 300 W was applied for 5 minutes. Furthermore, Qiu *et al.* (2023) studied the microwave-assisted pyrolysis of peanut shells. The outcomes reveal that the yields were 30.04 to 43.38 wt.% at a power level of 400-600 W for 1-3 hours. At 400 W for one hour, the highest yield was 43.38%. Furthermore, microwave pyrolysis was shown to generate more char and volatiles than other conventional pyrolysis techniques by choosing suitable operating conditions, consuming less time to finish.

3.4 EDX analysis and SEM of the biochar

The thermal transformation properties of biochar are critical in determining the mass change rate and thermochemical conversion. Fig. 5 and Table 2 show the preliminary analyses of biochar from *Dodonaea viscosa*. decomposition. The carbon content of biochar increased significantly from 51.3% to 89.69% when the power level was increased from 130 W to 650 W. Decarboxylation, dehydrogenation, and decarboxylation of cellulose biomass are the main reactions that happen when biomass is heated and broken down. All of these reactions lower the production of biochar. In contrast, the oxygen content decreased significantly, from 34.51% to 4.88%. Thus, biochar formed at a higher energy level has better chemical and physical properties than biochar formed at a lower energy level. The char produced by the deoxygenation process via thermal decomposition is a highly aromatic organic material (Hu, 2019).

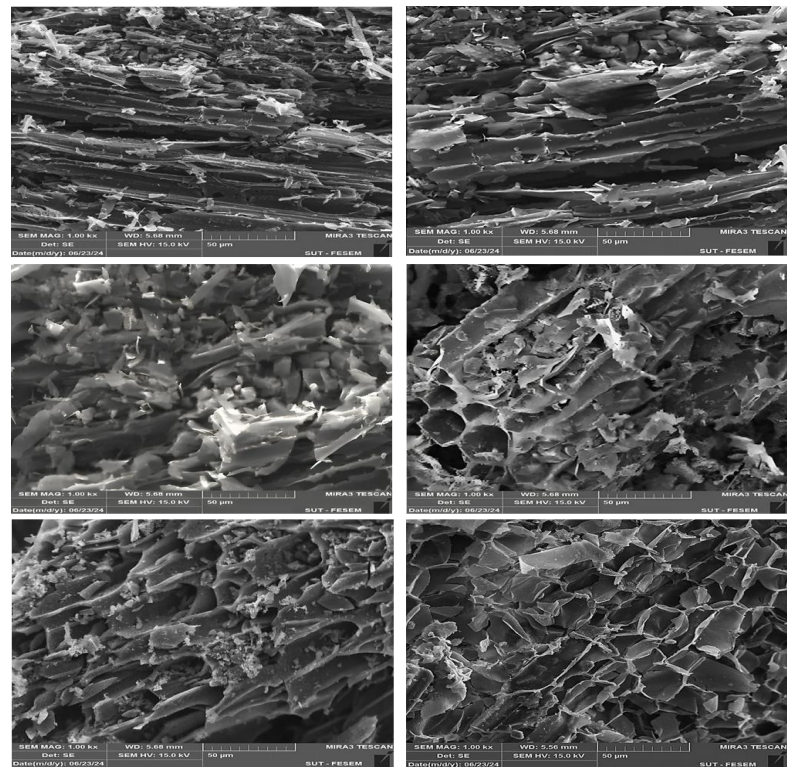


Fig 6. SEM of biochar and Dedonea branches at various power level A) Dedonea branches B)130 W C)260W D)390W E) 520W F)650W

This process also produces various volatile substances. Some of these substances can condense (such as acids and alcohols), but others cannot (such as carbon dioxide and carbon monoxide) (Chen *et al.*, 2019).

Figure 6 depicts the corresponding SEM images of *Dodonaea viscosa* biomass and biochar produced through microwave pyrolysis. The SEM clearly shows the biochar. Before heating, it did not appear to have any holes, but biochar made at 130 and 260 W had rough, uneven surfaces that could be seen in the stem cells (Figure 6 A and B). Furthermore, at 260 W of power, a few particles appeared on the surface of the biochar, resembling a group of grains. The SEM images also revealed the formation of new pores because of volatilization during the pyrolysis process, as shown in Figures 6C and 6E at power levels of 390 W and 520 W, respectively. When the power was increased to 650 W, the biochar exhibited exceptionally well-ordered honeycomb-like pores that were consistent with the literature (Xu *et al.*, 2021). SEM images also show how microwave energy affects the porosity of biochar. The pyrolysis process increases the microwave energy level, exposing the material's core layers. Cracks and pores appear when the layers are exposed. This is why the formation of the porous structure is primarily responsible for the release of volatile substances (Kumar *et al.*, 2018; Xu *et al.*, 2021).

3.5 FTIR (Fourier Transform Infrared Spectroscopy) analysis

FTIR analysis was used to analyze *Dodonaea v.*-derived biochar's changes in surface functional groups under various microwave power levels. Figure 7 and Table 3 show FTIR spectra of biochar produced with varying power levels with distinctive spectral changes indicative of chemical structure formation. Biochar produced with 130 W had distinctive absorption peaks at about 846.75, 910.40, 1367.53, 1450.46, 1535.33, 1924.95, 2553.14, 2906.01, and 3666.67 cm^{-1} . They are associated with groups such as C–H bending and stretching (aliphatic and aromatic), C–O stretching, C=O stretching in ketones and carbonyls, and broad O–H stretching for hydroxyl groups (Antonangelo *et al.*, 2019). Biochar exhibited a nearly similar spectral pattern at 260 W with peaks at 844.82, 908.47,

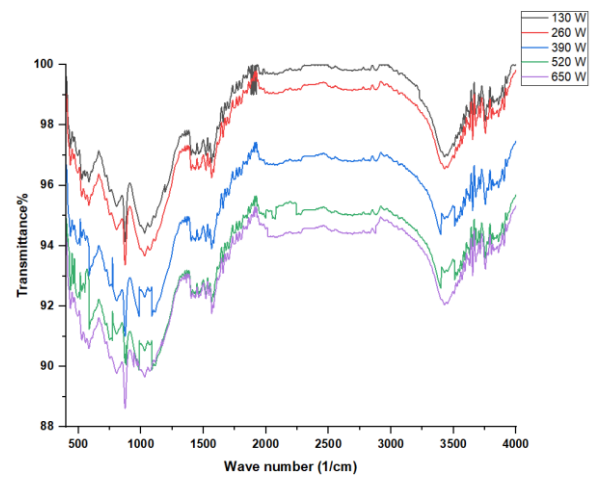


Fig. 7. The FTIR analysis of biochar and Dedonea branches at different Microwave power levels

1369.45, 1448.54, 1533.41, 1911.42, 2553.75, 2920.22, and 3664.75 cm^{-1} . Notably, the intensification of peaks associated with aromatic C=C bonds, O–H stretching, and C–O stretching is indicative of increased aromaticity and structure.

The strongest signal, marked by a peak at 1369.45 cm^{-1} for 260 W biochar during C=O stretching, suggests an increase in the presence of ketene or quinone groups, likely boosting the material's ability to undergo redox reactions and its surface activity, making it better for catalysis. Meanwhile, the O–H stretching band, which typically appears between 3250 and 3500 cm^{-1} , showed a drop in intensity as the microwave power went up. At the same time, the O–H stretching band, usually found between 3250 and 3500 cm^{-1} , showed a decrease in intensity as microwave power increased. At the same time, the O–H stretching band, usually found between 3250 and 3500 cm^{-1} , showed a greater decrease in intensity as the microwave power increased. Normalized transmittance values, which range from 99.14 to 94.51 a.u., also support this. The drop shows that –OH groups are taken away because of dihydroxylation, which

Table 3
Functional groups of Fourier Transform Infrared (FTIR)

Functional Group	Wavenumber, cm^{-1} (Normalized Transmittance)					reference
	130W	260W	390W	520W	650W	
O–H stretching (3700 to 3600)	3666.67 (99.14)	3664.75 (99.01)	3666.15 (96.66)	3664.75 (94.88)	3674.7 (94.51)	Dai <i>et al.</i> , (2023)
C–H stretching in aliphatic formation (2960–2850)	2906.01 (99.98)	2920.22 (99.44)	2914.44 (97.07)	2916.36 (95.31)	2918.29 (94.94)	Antonangelo <i>et al.</i> (2019), Reza <i>et al.</i> (2019b)
C–H Bending in aliphatic formation (2830–2670)	2553.14 (99.94)	2553.75 (99.29)	2555.65 (96.93)	2557.61 (95.15)	2551.8 (94.54)	Antonangelo <i>et al.</i> (2019)
C=O stretching in ketene groups (2350–1910)	1924.95 (99.98)	1911.42 (99.78)	1913.38 (97.42)	1923.029 (95.61)	1924.95 (95.25)	Reza <i>et al.</i> (2019a)
C=C stretching of hemicelluloses (1610–1510)	1535.33 (97.94)	1533.41 (97.07)	1535.33 (94.64)	1533.408 (92.99)	1533.408 (92.93)	Popescu <i>et al.</i> (2018)
C–H deformation in cellulose and hemicellulose (1480–1410)	1450.46 (97.39)	1448.54 (96.86)	1448.54 (94.45)	1446.72 (92.73)	1448.51 (92.76)	Traoré <i>et al.</i> (2015), Tayibi <i>et al.</i> (2020)
C–H bending (1365–1380)	1367.53 (97.82)	1369.45 (97.31)	1371.33 (94.95)	1379.103 (93.12)	1367.5 (93.03)	Antonangelo <i>et al.</i> (2019)
C–O stretching vibration in cellulose and hemicelluloses (1120–1050)	-	-	1052.025 (92.06)	1060.24	1055.77 (89.96)	Popescu <i>et al.</i> (2018), Reza <i>et al.</i> (2019a)
C–O stretching in cellulose (995–905)	910.401 (90.55)	908.472 (95.29)	908.47 (92.91)	912.601 (91.16)	914.359 (90.54)	Traoré <i>et al.</i> (2015), Popescu <i>et al.</i> (2018)
Aromatic rings (880–720)	846.75 (95.67)	844.82 (94.89)	850.6 (92.47)	846.92 (91.44)	844.821 (90.15)	Antonangelo <i>et al.</i> (2019)

reduces the polarity of biochar and its ability to take in polar substances like heavy metals and certain organic pollutants. These structural and chemical changes have far-reaching consequences for biochar's functional properties. The presence of aromatic C–H and C=C bonds ($846\text{--}910\text{ cm}^{-1}$ and $1367\text{--}1535\text{ cm}^{-1}$) makes biochar more stable at high temperatures and helps it last longer in storing carbon, which is important for keeping carbon in the ground for a long time. This stability is also useful when adding biochar to soil, as it resists breaking down by microbes. These aromatic functions also help attract and hold onto water-soluble organic pollutants during water cleanup, making biochar better at absorbing these harmful substances. On the other hand, losing O–H groups would affect biochar's ability to improve soil, since these groups help hold onto water and nutrients through hydrogen bonding and cation exchange capacity. Having fewer hydrophilic groups can be beneficial for using biochar to clean up contaminants in organic solvents because it reduces attraction to water.

Besides, the addition of more C–O and C=O groups increase biochar's chemical activity, providing active sites for catalytic reactions, such as higher-order oxidation reactions or metal cation anchoring sites for use as supports for metal catalysts. These oxygen groups help hold onto heavy metal cations and are important for how well biochar works in cleaning up the environment, like in capturing lead (Pb^{2+}), cadmium (Cd^{2+}), or arsenic (As^{5+}) (Dai *et al.*, 2023). So, the changes made to biochar using FTIR not only show how its chemical structure changes with more microwave power, but also how it can be used for different purposes like adsorption, catalysis, carbon sequestration, and improving soil.

3.6 XRD of the biochar

The scanning electron microscope images of *Dodonaea viscosa* branches before and after pyrolysis are shown in Figures 8-A and 8-B, clearly showing the changes that happened because of microwave-assisted pyrolysis. The images also show a noticeable difference in the porosity and surface structure of the biomass, highlighting the impact of microwave energy on the plant's shape. The micrographs also reflect sharp contrast in biomass porosity and surface morphology, which is indicative of microwave energy's effect upon plant morphology. Figure 8 also shows raw biomass and the biochar product's X-ray diffraction pattern, which clearly demonstrates differences in the types of materials and their crystal structure. The diffraction patterns show that the clear peaks of the crystals become less sharp and wider, particularly for cellulose. The change indicates

a shift from a neatly arranged carbon structure to a more chaotic one. This semi-quantitative evolution is reflected in the decreased intensity of peaks along with the increased full width at half maximum (FWHM) of crystalline cellulose reflections with increasing microwave power. The result is realized through thermal decomposition of lignocellulosic components, where volatiles are pushed out, polymer side chains are cleaved, intra- and intermolecular hydrogen bonding is destroyed, and the order of crystals is diminished (Cheng *et al.*, 2021; Bielecki *et al.*, 2023).

As pyrolysis progresses, the loss of oxygen and hydrogen atoms breaks down hemicellulose, cellulose, and lignin into smaller parts. Such disintegration induces amorphous carbon formation, being abundant in aliphatic chains as well as aromatic ring systems—primarily from hemicellulose and lignin fractions. Greater energy provision results in such aromatic subunits condensing to form conjugated polyaromatic sheets that are transformed to an amorphous, graphitic-like matrix with disordered layered carbon structure (Sadegh *et al.*, 2023; Widayat *et al.* 2017). The biochar-formed XRD pattern at 650 W, as shown in Figure 8-B, consists of a diffuse hump in the range of about 19.5° to 24.0° in 2θ , which is due to disordered carbon's (002) reflection. The peak represents turbostratic layers of carbon with partial aromatic order, which is one of the common features of pyrolyzed biomass. In the range of 42.2° to 46.8° , there is another bump that is linked to the (100) plane, which displays features of aromatic rings and the growth of side crystals (Pusceddu *et al.*, 2017).

Changing to an amorphous carbon form greatly affects the physical and chemical properties and uses of the resulting biochar. The amorphous carbon forms have a larger surface area and more pores, which are beneficial for capturing substances, speeding up chemical reactions, and improving soil quality. The uneven pore structure and higher number of active sites in amorphous forms allow them to trap water, nutrients, and pollutants, making the material more useful in the environment. The creation of the amorphous phase also results in the formation of carboxyl, hydroxyl, and carbonyl groups, which enhance how the biochar reacts chemically and interacts with its surroundings. The amorphous carbon is also more resistant to microbial attack relative to their crystalline counterparts, as reflected through increased carbon persistence with longer residence in soil environments (Sadegh *et al.*, 2023). Therefore, change in structure revealed by XRD portrays the multifaceted advantage of amorphization in microwave pyrolysis, making the applicability of *Dodonaea v.*-derived

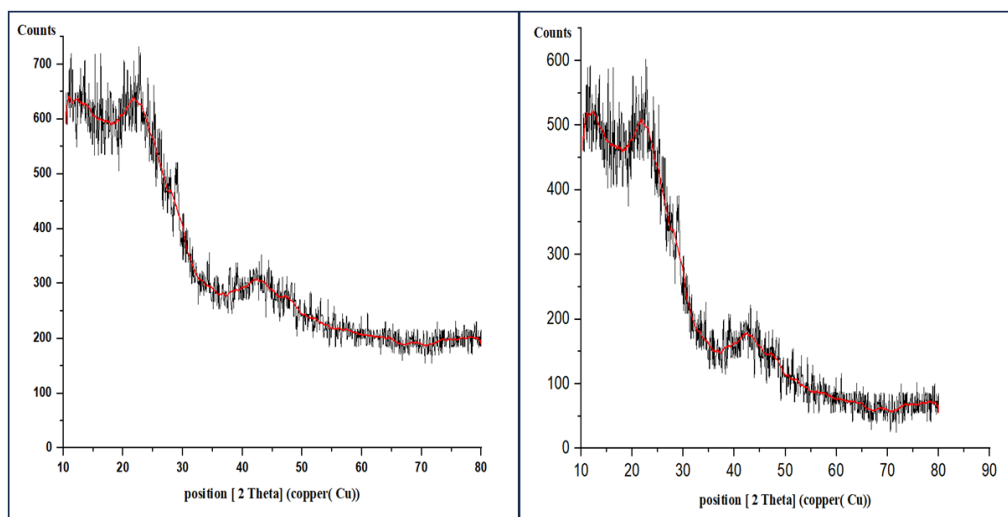


Fig. 8. XRD analysis of A) *Dodonaea* branches before pyrolysis B) pyrolyzed at 650 W

Table 4
Yield and pore specification of the biochar.

Samples	S _{BET} ^a (m ² /g)	S _{Micro} ^b (m ² /g)	V _{Tot} ^c (cm ³ /g)	r _p (nm)	Yield %
BC130	3.0436	1.7352	0.008124	13.215	43.43
BC260	9.8157	6.0708	0.026299	10.717	38.94
BC390	12.1487	10.8731	0.03794	7.652	33.725
BC520	21.634	16.9785	0.03522	4.871	27.58
BC650	17.0229	13.4624	0.038231	2.653	25.67

^a The total area assessed within the pressure range of 0.05 < P/P₀ < 0.1.
^b Micro-pore surface area plotted using t-plot.
^c The Total Pore Volume (V_{Tot}) is determined by calculating the liquid's volume at a pressure of P/P₀=0.990.
^d Average pore diameter (radial diameter)

biochar to a wide range of applications in the environment as well as in industry.

3.7 Studies of Surface Area and Pore Volume of Biochar

Using an N₂ adsorption/desorption analyzer, Table 4 shows the surface area, average pore size, and pore volume of the biochar that was made. The BET of biochar made from *Dodonaea viscosa*. branches using microwaves at different power levels was 3.0436, 9.8157, 12.1487, 21.634, and 17.0229 m²/g. At 520 W, the maximum surface area was 21.634. It was discovered that increasing the power level enhanced the pore structure of biochar. As the power level increased from 130 W to 650 W (carbonization temperature), larger molecules were mobilized, and the volume of the volatile molecules gradually decreased, whereas the release of smaller molecules enhanced the micropores in the sample, increasing the BET surface area. These findings were consistent with those of Oginni and Singh (2020), who found that BET surface area and micropore volume improved as temperature increased. When it was heated up, big holes and open patterns appeared on the surface. These features made it easier for volatile substances to escape (Oginni & Singh, 2020). The biochar made by microwave pyrolysis had a larger BET surface area and pore volume than most biochar made by traditional pyrolysis (Zhang *et al.*, 2022). Traditional heating methods change energy into heat and then move it from the surface to the core of the material through changes in temperature. Microwaves, on the other hand, heat at the molecular level by directly changing electromagnetic energy into heat and moving heat from the inside to the outside of the biomass radiation. Microwave radiation may be a useful method to modify the surface area and pore size distribution (Zhang *et al.*, 2022). In addition, as the microwave power level went up, the total pore volume went from 0.008124 cm³/kg to 0.038231 cm³/kg, while the pore diameter went down from 13.215 nm to 2.653 nm, showing that there were more pores. The content of volatile components in the raw material significantly affects the structure of the formed biochar. This procedure is an example of how to make biochar with low volume and high pores using very volatile substances, like CH₄ and H₂. The observed phenomena can successfully explain the reason behind the negative correlation between biochar yield and thermal acids (Oginni & Singh 2020).

Nevertheless, the determined surface area started to decline when the power level increased above 520 W. The decreases in

S_{BET} values seem to be due to the pore volume integration process that leads to pore widening/merging of adjacent pores. There were smaller and smaller pores in the amorphous structures of monoclinic carbons as the energy level dropped (13.215, 10.717, 7.652, 4.871, 2.653 nm). This phenomenon means that the amorphous carbon structure changes into the microcrystalline graphite structure (Zhang *et al.*, 2015a). Melting, coalescence, softening, and carbonizations affect pores locally. These steps would stop the volatile substances that were adsorbed from moving into the pores during the combined process, which would get rid of some of the surface area. To compare this outcome with existing literature, Table 5 presents the effect of power levels on the BET surface area of various feedstocks. The BET surface area of *Dodonaea viscosa* biochar made with microwave-assisted pyrolysis (520 W, 25 min) was 21.634 m²/g, showing it has a moderate number of pores and surface area. Compared to other biomass feedstocks, rice husk produced the highest surface area in terms of 172.04 m²/g at 1000 W for 5 min (Kuo *et al.*, 2023), with an indication of excellent pore development at an elevated energy input. Biochar produced by pyrolysis of cow dung at 800 W for 5 min attained 127 m²/g (Tsai *et al.*, 2023) with an indication of a high surface area due to volatile-rich organic content. Peanut shells also attained 67.29 m²/g at 500 W with an extended time of 120 min (Qiu *et al.*, 2023), indicating the ability of longer residence time to drive the impact of moderate power. Wood chips produced a relatively lower surface area of 20.5 m²/g at only 36 W with a longer time of 20 min (Fernández *et al.*, 2024) and make *Dodonaea viscosa*. superior under comparable conditions of less power. *Dodonaea viscosa* cannot match the level of surface area that can be generated by high-energy systems, but its steady response under moderate power and time provides confidence that *Dodonaea viscosa* is a sustainable and scalable feedstock material with room for further improvement with the addition of a catalyst or with process optimization.

3.8 Comparative with literature

Microwave-assisted pyrolysis (MAP) shows better results than conventional pyrolysis (CP). Table 6 clearly shows the performance of the biochar from various biomass sources processed by microwave-assisted pyrolysis (MAP) and conventional pyrolysis (CP). The table represents the important parameters—biochar yield, surface area, and consumed energy—that are used to identify the efficacy and feasibility of

Table 5
The effect of power level on the BET for various biomass-derived biochar

Biomass Source	Microwave Power (W)	Residence Time (min)	BET Surface Area (m ² /g)	Reference
Rice husk	1000	5	172.04	Kuo <i>et al.</i> , 2023
Cow dung	800	5	127	Tsai <i>et al.</i> , 2023
Peanut shell	500	120	67.29	Qiu <i>et al.</i> , 2023
Wood Chips	36	20	20.5	Fernández <i>et al.</i> , 2024
<i>Dedonea</i> branches	520	25	21.634	[current Study]

Table 6
Comparative Analysis of Biochar produced from Different Pyrolysis Methods and Feedstocks

Biomass Feedstock	Pyrolysis Method	Biochar Yield (%)	Surface Area (m ² /g)	Energy Consumption (kJ/g)	References
Peanut Shell	Microwave-Assisted	30.04–43.38	67.29	Not specified	Qiu <i>et al.</i> , 2023
Rice Husk	Conventional	25–31	10.3–18.4	~3.0	Tsai <i>et al.</i> , 2006
Corn Stover	Conventional	27–33	5.0–10.2	2.7–3.1	Ahmad <i>et al.</i> , 2012
Sugarcane Bagasse	Conventional	28–32	8.4–13.7	2.9–3.2	Zafeer <i>et al.</i> , 2024
Wood Chips	Microwave-Assisted	32–36	15.2–20.5	1.5–2.2	Fernández <i>et al.</i> , 2024
Corn Straw	Conventional	Not specified	4.62–20.96	Not specified	Qiu <i>et al.</i> , 2023
<i>Dodonaea viscosa</i>	Microwave-Assisted	30–35	21.63	1.07–2.5	current study

each process. The Conventional Pyrolysis (CP) of different materials like corn stover (Qiu *et al.*, 2023), sugarcane bagasse (Zafeer *et al.*, 2024), and rice husks (Tsai *et al.*, 2006), results in smaller surface areas, typically under 20 m²/g, and requires more energy, around 2.7 to 3.2 kJ/g. These are due to the poorer heat transfer and longer residence times in CP. Rice husks and sugarcane bagasse, for instance, although they are found in abundance, form comparatively low surface area biochar that are higher in energy demand, limiting their use in challenging applications such as in the fields of catalysis or water treatment. In contrast, microwave-assisted pyrolysis (MAP) is extremely effective. *Dodonaea viscosa*, the subject of the work in hand, had 30–35% biochar of 21.63 m²/g surface area and a very low range of 1.07–2.5 kJ/g for utilization of energy. These are in comparison to other MAP precursors, including peanut shells and wood chips. Peanut shells were of greater surface area (67.29 m²/g), i.e., they were more porous with the potential to be of greater capacity to adsorb, although their utilization of the energy component in the data was not available. Wood chips (Guo *et al.*, 2023), on the other hand, had similar yields (32–36%) and low readings of the surface area (15.2–20.5 m²/g) with similar utilization of the energy (1.5–2.2 kJ/g). The inclusion of the drought-resistant, hardy plant *Dodonaea viscosa* in this study increases its value by offering a renewable source of biomass that can be used in dry environments. Its MAP-derived biochar has a balanced performance that supports its potential application in adsorption, carbon sequestration, and conditioning of the soil while sustaining energy efficiency and moderate structural porosity. In general, the table supports the benefits of MAP for high-quality biochar production with better surface properties and low energy requirements. The table also supports *Dodonaea viscosa* as a suitable feedstock for future large-scale biochar production, particularly in a resource-limited or stressed environment.

6. Conclusion

In this study, *Dodonaea viscosa* branches were pyrolyzed to biochar via microwave-assisted pyrolysis (MAP) to analyze the effect of power, particle size, and time. Higher power and small particle size were found to enhance surface area and pore size and alter the structure to amorphous. For instance, at 520 W for 25 min, the surface area was nearly sevenfold increased and carbon content was 89.7%, corresponding to increased carbonization. The maximum yield of biochar (43.43 wt.%) was found at 130 W, while larger powers were favorable to the production of bio-oil and gas and porosity. The maximum surface area (21.63 m²/g) was seen at 550 W. MAP biochar also had a better BET surface area of 3.03–21.63 m²/g compared to CP, at 5–12 m²/g. In addition, MAP reduced the time and energy demand (6–15 min compared to 30–60 min in CP) and made the process more efficient and scalable, with a demand of 1.07–2.5 kJ/g compared to 2.7–3.1

kJ/g. Biochar production from *Dodonaea* is similar (30-35%) to that of amorphous carbon, as demonstrated by XRD, due to the increased reactivity and adsorptivity. FTIR identified functional groups responsible for purification of water, nutrient holding, and catalysis (O–H, C=O, C–O). Emission of CO₂ was also reduced by MAP as compared to CP, confirming its environmental friendliness. *Dodonaea viscosa* was identified to be a superior biomass to yield quality biochar by MAP.

Acknowledgements

This study was partially supported by College of Engineering, Baghdad University and the College of Engineering, Tikrit University, Iraq.

Contributions: The authors contributed to the study's conception and design. Material preparation, data collection, and analysis were performed by [Safa W. SHAKIR] and [Atheer M. Al-YAQOOBI]. The first draft of the manuscript was written by [Safa W. SHAKIR], and [Atheer M. Al-YAQOOBI] commented on previous versions of the manuscript. The authors read and approved the final manuscript.

Funding: The author(s) received no financial support for the research, authorship, and/or publication of this article.

Conflict of interest: The authors declare that they have no known competing financial interests or personal relationships that could have appeared to influence the work reported in this paper.

References

Abbas, A. S., Ahmed, M. J., & Darweesh, T. M. (2016). Adsorption of fluoroquinolones antibiotics on activated carbon by K2CO3 with microwave assisted activation. *Iraqi Journal of Chemical and Petroleum Engineering*, 17(2), 15-23. <https://doi.org/10.31699/IJCPE.2016.2.3>

Abd, M. F., & Al-Yaqoobi, A. M. (2023). The feasibility of utilizing microwave-assisted pyrolysis for Albizia branches biomass conversion into biofuel productions. *International Journal of Renewable Energy Development*, 12(6). <https://doi.org/10.14710/ijred.2023.56907>

Abd, M. F., & AL-yaqoobi, A. M. (2025). The potential significance of microwave-assisted catalytic pyrolysis for valuable bio-products driven from Albizia tree. *Applied Science and Engineering Progress*, 18(1), 7454-7454. <https://doi.org/10.14416/jasep.2024.07.016>

Abd, M. F., Al-yaqoobi, A. M., & Abdul-Majeed, W. S. (2024). Catalytic microwave pyrolysis of Albizia Branches using iraqi bentonite clays. *Iraqi Journal of Chemical and Petroleum Engineering*, 25(2), 175-186. <https://doi.org/10.31699/IJCPE.2024.2.16>

Ahmed, M. J. (2019). Enhanced conversion of Glycerol-to-Glycerol carbonate on modified Bio-Char from reed plant. *Iraqi Journal of Chemical and Petroleum Engineering*, 20(4), 15-20. <https://doi.org/10.31699/IJCPE.2019.4.3>

Ahmad, M., Lee, S. S., Dou, X., Mohan, D., Sung, J. K., Yang, J. E., & Ok, Y. S. (2012). Effects of pyrolysis temperature on soybean stover- and peanut shell-derived biochar properties and TCE adsorption

- in water. *Bioresource technology*, 118, 536-544. <https://doi.org/10.1016/j.biortech.2012.05.042>
- Antonangelo JA, Zhang H, Sun X, Kumar A (2019) Physicochemical properties and morphology of biochar as affected by feedstock sources and pyrolysis temperatures. *Biochar* 1:325–336. <https://doi.org/10.1007/s42773-019-00028-z>
- Azni, A. A., Ghani, W. A. W. A. K., Idris, A., Ja'afar, M. F. Z., Salleh, M. A. M., & Ishak, N. S. (2019). Microwave-assisted pyrolysis of EFB-derived biochar as potential renewable solid fuel for power generation: Biochar versus sub-bituminous coal. *Renewable Energy*, 142, 123-129. <https://doi.org/10.1016/j.renene.2019.04.035>
- Bielecki, M., & Zubkova, V. (2023). Analysis of interactions occurring during the pyrolysis of lignocellulosic biomass. *Molecules*, 28(2), 506. <https://doi.org/10.3390/molecules28020506>
- Campbell, R. M., Anderson, N. M., Daugaard, D. E., & Naughton, H. T. (2018). Financial viability of biofuel and biochar production from forest biomass in the face of market price volatility and uncertainty. *Applied energy*, 230, 330-343. <https://doi.org/10.1016/j.apenergy.2018.08.085>
- Castañeda-Espinoza, J., Salinas-Sánchez, D. O., Mussali-Galante, P., Castrejón-Godínez, M. L., Rodríguez, A., González-Cortazar, M., ... & Tovar-Sánchez, E. (2023). *Dodonaea viscosa* (Sapindaceae) as a phytoremediator for soils contaminated by heavy metals in abandoned mines. *Environmental Science and Pollution Research*, 30(2), 2509-2529. <https://doi.org/10.1007/s11356-022-22374-5>
- Chen W (2019) Inaugural editorial: pioneering the innovation and exploring the future for biochar technology. *Biochar* 1, 1–1. <https://doi.org/10.1007/s42773-019-00010-9>
- Chen, C., Yang, L., Zhang, X., Zhao, C., Sun, J., Li, G., & Shi, H. (2024). Advances and prospects of multifunctional biochar-based materials from organic solid waste of traditional Chinese medicine: A review. *Biomass and Bioenergy*, 187, 107296. <https://doi.org/10.1016/j.biombioe.2024.107296>
- Cheng, J., Hu, S. C., Sun, G. T., Geng, Z. C., & Zhu, M. Q. (2021). The effect of pyrolysis temperature on the characteristics of biochar, pyrolytic acids, and gas prepared from cotton stalk through a polygeneration process. *Industrial Crops and Products*, 170, 113690. <https://doi.org/10.1016/j.indcrop.2021.113690>
- Conte, P., Bertani, R., Sgarbossa, P., Bambina, P., Schmidt, H. P., Raga, R., ... & Lo Meo, P. (2021). Recent developments in understanding biochar's physical chemistry. *Agronomy*, 11(4), 615. <https://doi.org/10.3390/agronomy11040615>
- Dai, F., Zhuang, Q., Huang, G., Deng, H., & Zhang, X. (2023). Infrared spectrum characteristics and quantification of OH groups in coal. *ACS omega*, 8(19), 17064-17076. <https://doi.org/10.1021/acsomega.3c01336>
- Do Nascimento, V. R., dos Santos, M. B., Diehl, L., Paniz, J. N. G., de Castilhos, F., & Bizzi, C. A. (2024). Microwave-assisted pyrolysis of pine wood waste: system development, biofuels production, and characterization. *Journal of Analytical and Applied Pyrolysis*, 106799. <https://doi.org/10.1016/j.jaap.2024.106799>
- Fan, S., Cui, L., Li, H., Guang, M., Liu, H., Qiu, T., & Zhang, Y. (2023). Value-added biochar production from microwave pyrolysis of peanut shell. *International Journal of Chemical Reactor Engineering*, 21(8), 1035-1046. <https://doi.org/10.1515/ijcre-2023-0005>
- Fernández, I., Pérez, S. F., Fernández-Ferreras, J., & Llano, T. (2024). Microwave-assisted pyrolysis of forest biomass. *Energies*, 17(19), 4852. <https://doi.org/10.3390/en17194852>
- Guo, H., Qin, X., Cheng, S., Xing, B., Jiang, D., Meng, W., & Xia, H. (2023). Production of high-quality pyrolysis product by microwave-assisted catalytic pyrolysis of wood waste and application of biochar. *Arabian Journal of Chemistry*, 16(8), 104961. <https://doi.org/10.1016/j.arabjc.2023.104961>
- Hadiyanto, H., Azimatun Nur, M. M., & Hartanto, G. D. (2012). Cultivation of *Chlorella* sp. as Biofuel Sources in Palm Oil Mill Effluent (POME). *International Journal of Renewable Energy Development*, 1(2), 45-49
- Jamilatun, S., Budhijanto, B., Rochmadi, R., Yuliestyan, A., Hadiyanto, H., & Budiman, A. (2019). Comparative analysis between pyrolysis products of *Spirulina platensis* biomass and its residues. *International Journal of Renewable Energy Development*, 8(2), 133-140. <https://doi.org/10.14710/ijred.8.2.133-140>
- Ke, L., Zhou, N., Wu, Q., Zeng, Y., Tian, X., Zhang, J., ... & Wang, Y. (2024). Microwave catalytic pyrolysis of biomass: a review focusing on absorbents and catalysts. *npj Materials Sustainability*, 2(1), 24. <https://doi.org/10.1038/s44296-024-00027-7>
- Khelfa, A., Rodrigues, F. A., Koubaa, M., & Vorobiev, E. (2020). Microwave-assisted pyrolysis of pine wood sawdust mixed with activated carbon for bio-oil and bio-char production. *Processes*, 8(11), 1437. <https://doi.org/10.3390/pr8111437>
- Khawkomol, S., Neamchan, R., Thongsamer, T., Vinitnantharat, S., Panpradit, B., Sohsalam, P., ... & Mrozik, W. (2021). Potential of biochar derived from agricultural residues for sustainable management. *Sustainability*, 13(15), 8147. <https://doi.org/10.3390/su13158147>
- Kumar, A., Joseph, S., Tsechansky, L., Privat, K., Schreiter, I. J., Schüth, C., & Graber, E. R. (2018). Biochar aging in contaminated soil promotes Zn immobilization due to changes in biochar surface structural and chemical properties. *Science of the Total Environment*, 626, 953-961. <https://doi.org/10.1016/j.scitotenv.2018.01.157>
- Kumar, D., Yadav, K. K., & Gupta, N. (2022). Phytoremediation potential of *Dodonaea v.*: A sustainable approach to metal-contaminated soils. *Environmental Science and Pollution Research*, 29, 23456–23468. <https://doi.org/10.1007/s11356-022-22374-5>
- Kuo, L. A., Tsai, W. T., Yang, R. Y., & Tsai, J. H. (2023). Production of high-porosity biochar from rice husk by the microwave pyrolysis process. *Processes*, 11(11), 3119. <https://doi.org/10.3390/pr11113119>
- Lehmann, J., Rillig, M. C., Thies, J., Masiello, C. A., Hockaday, W. C., & Crowley, D. (2021). Biochar effects on soil biota – A review. *Soil Biology and Biochemistry*, 43(9), 1812–1836. <https://doi.org/10.1016/j.soilbio.2011.04.022>
- Lehmann, J., & Joseph, S. (2015). *Biochar for Environmental Management: Science, Technology and Implementation*. Routledge. <https://doi.org/10.4324/9780203762264>
- Li, J., Dai, J., Liu, G., Zhang, H., Gao, Z., Fu, J., ... & Huang, Y. (2016). Biochar from microwave pyrolysis of biomass: A review. *Biomass and Bioenergy*, 94, 228-244. <https://doi.org/10.1016/j.biombioe.2016.09.010>
- Li, J., Lin, L., Ju, T., Meng, F., Han, S., Chen, K., & Jiang, J. (2024). Microwave-assisted pyrolysis of solid waste for production of high-value liquid oil, syngas, and carbon solids: A review. *Renewable and Sustainable Energy Reviews*, 189, 113979. <https://doi.org/10.1016/j.rser.2023.113979>
- Li, X., Peng, B., Liu, Q., & Zhang, H. (2022). Microwave pyrolysis coupled with conventional pre-pyrolysis of the stalk for syngas and biochar. *Bioresource Technology*, 348, 126745. <https://doi.org/10.1016/j.biortech.2022.126745>
- Liu, L., Gou, G., Liu, J., Zhang, X., Zhu, Q., Mou, J., ... & He, Q. (2022). Effects of *Dodonaea v.* afforestation on soil nutrients and aggregate stability in Karst Graben Basin. *Land*, 11(8), 1140. <https://doi.org/10.3390/land11081140>
- Lin, J., Ma, R., Luo, J., Sun, S., Cui, C., Fang, L., & Huang, H. (2020). Microwave pyrolysis of food waste for high-quality syngas production: Positive effects of a CO₂ reaction atmosphere and insights into the intrinsic reaction mechanisms. *Energy Conversion and Management*, 206, 112490. <https://doi.org/10.1016/j.enconman.2020.112490>
- Liu, C., Qiu, T., Mostafa, E., Liu, H., Zhao, W., & Zhang, Y. (2024). Porous biochar production from pyrolysis of corn straw in a microwave heated reactor. *International Journal of Chemical Reactor Engineering*, 22(3), 267-276. <https://doi.org/10.1515/ijcre-2023-0128>
- Lu, H., Xie, R., Almoallim, H. S., Alharbi, S. A., Jhanani, G. K., Praveenkumar, T. R., ... & Xia, C. (2023). Utilization of the *Nannochloropsis* microalgae biochar prepared via microwave assisted pyrolysis on the mixed biomass fuel pellets. *Environmental Research*, 231, 116078. <https://doi.org/10.1016/j.envres.2023.116078>
- Mahmood, S. S., & Al-Yaqoobi, A. M. (2024). Production of biodiesel by using CaO nano-catalyst synthesis from mango leaves extraction. *International Journal of Renewable Energy Development*, 13(6), 1025-1034. <https://doi.org/10.61435/ijred.2024.60469>

- Mahmood, S. S., & AL-Yaqoobi, A. M. (2025). Microwave assisted production of biodiesel using CaO nano-catalyst produced from mango fallen leaves extract. *Journal of Ecological Engineering*, 26(1). <https://doi.org/10.12911/22998993/195650>
- Majeed, N. S., Sabbar, H. A., & Al-Musawi, N. O. (2017). Preparation activated carbon from scrap tires by microwave assisted KOH activation for removal emulsified oil. *Iraqi Journal of Chemical and Petroleum Engineering*, 18(1), 57-69.
- Neha S, Rajput P, Remya N. Biochar from microwave co-pyrolysis of food waste and polyethylene using different microwave susceptors - Production, modification and application for metformin removal. *Environ Res*. 210, 112922. <https://doi.org/10.1016/j.envres.2022.112922>
- Oginni, O., & Singh, K. (2020). Influence of high carbonization temperatures on microstructural and physicochemical characteristics of herbaceous biomass derived biochar. *Journal of Environmental Chemical Engineering*, 8(5), 104169. <https://doi.org/10.1016/j.jece.2020.104169>
- Paikamnam, A., Clowutimon, W., Chanpee, S., Sriprom, P., & Assawasaengrat, P. (2021, September). Production of empty palm bunch biochar using microwave-assisted pyrolysis at low temperature. *AIP Conference Proceedings*, 2397(1). AIP Publishing. <https://doi.org/10.1063/5.0064053>
- Patwardhan, S. B., Pandit, S., Gupta, P. K., Jha, N. K., Rawat, J., Joshi, H. C., ... & Kesari, K. K. (2022). Recent advances in the application of biochar in microbial electrochemical cells. *Fuel*, 311, 122501. <https://doi.org/10.1016/j.fuel.2021.122501>
- Popescu C, Popescu M, Singurel G et al (2018) Spectral characterization of eucalyptus wood. *Soc Appl Spectrosc* 61:1–17. <https://doi.org/10.1366/00037020782597076>
- Potnuri, R., & Rao, C. S. (2024). Synthesis and Characterization of Biochar Obtained from Microwave-Assisted Copyrolysis of Torrefied Sawdust and Polystyrene. *ACS Sustainable Resource Management*, 1(9), 2074-2085. <https://doi.org/10.1021/acssusresmg.4c00195>
- Pusceddu, E., Montanaro, A., Fioravanti, G., Santilli, S. F., Foscolo, P. U., Criscuoli, I., ... & Miglietta, F. (2017). Comparison between ancient and fresh biochar samples, a study on the recalcitrance of carbonaceous structures during soil incubation. *Int. J. New Technol. Res*, 3, 39-46.
- Qiu, T., Li, C., Guang, M., & Zhang, Y. (2023). Porous carbon material production from microwave-assisted pyrolysis of peanut shell. *Carbon Research*, 2(1), 45. <https://doi.org/10.1007/s44246-023-00079-9>
- Qiu, T., Liu, C., Cui, L., Liu, H., Muhammad, K., & Zhang, Y. (2023). Comparison of corn straw biochar from electrical pyrolysis and microwave pyrolysis. *Energy Sources, Part A: Recovery, Utilization, and Environmental Effects*, 45(1), 636-649. <https://doi.org/10.1080/15567036.2023.2172484>
- Quillope, J. C. C., Carpio, R. B., Gatdula, K. M., Detras, M. C. M., & Doliente, S. S. (2021). Optimization of process parameters of self-purging microwave pyrolysis of corn cob for biochar production. *Heliyon*, 7(11). <https://doi.org/10.1016/j.heliyon.2021.e08417>
- Reza MS, Ahmed A, Caesarendra W et al (2019a) Acacia Holosericea : an invasive species for bio-char, bio-oil and biogas production. *Bioengineering*, 6, 33. <https://doi.org/10.3390/bioengineering6020033>
- Reza MS, Islam SN, Afroze S et al (2019b) Evaluation of the bioenergy potential of invasive Pennisetum purpureum through pyrolysis and thermogravimetric analysis. *Energy, Ecol Environ*. <https://doi.org/10.1007/s40974-019-00139-0>
- Sadegh, F., Sadegh, N., Wongniramaikul, W., Apiratikul, R., & Choodum, A. (2023). Adsorption of volatile organic compounds on biochar: A review. *Process Safety and Environmental Protection*. <https://doi.org/10.1016/j.psep.2023.11.071>
- Sandhya Rani, M., Pippalla, R. S., & Mohan, K. (2009). Dodonaea v. Linn.an overview. *Asian J. Pharm. Res. Healthcare*, 1, 97-112. <http://api.semanticscholar.org>
- Siipola, V., Pflugmacher, S., Romar, H., Wendling, L., & Koukari, P. (2020). Low-cost biochar adsorbents for water purification including microplastics removal. *Applied sciences*, 10(3), 788. <https://doi.org/10.3390/app10030788>
- Shakir, S. W., Hussein, S. S., Khazaal, S. H., Al-Naseri, H. A., Ahmed, A. M., Hachim, R. N., & Al-Dahhan, M. H. (2024). Examination and Improvement of the Taguchi-Based Nanofluids Impact on CO2 Absorption using Al2O3 Nanoparticles. *Journal of Advanced Research in Fluid Mechanics and Thermal Sciences*, 120(1), 204–216. <https://doi.org/10.37934/arfmts.120.1.204216>
- Shi, K., Yan, J., Menéndez, J. A., Luo, X., Yang, G., Chen, Y., ... & Wu, T. (2020). Production of H2-rich syngas from lignocellulosic biomass using microwave-assisted pyrolysis coupled with activated carbon enabled reforming. *Frontiers in chemistry*, 8, 3. <https://doi.org/10.3389/fchem.2020.00003>
- Song, B., Almatrafi, E., Tan, X., Luo, S., Xiong, W., Zhou, C., ... & Gong, J. (2022). Biochar-based agricultural soil management: An application-dependent strategy for contributing to carbon neutrality. *Renewable and Sustainable Energy Reviews*, 164, 112529. <https://doi.org/10.1016/j.rser.2022.112529>
- Suresh, A., Alagusundaram, A., Kumar, P. S., Vo, D. V. N., Christopher, F. C., Balaji, B., ... & Sankar, S. (2021). Microwave pyrolysis of coal, biomass and plastic waste: a review. *Environmental Chemistry Letters*, 19, 3609-3629.
- Tan, X., Liu, Y., Zeng, G., Wang, X., Hu, X., Gu, Y., & Yang, Z. (2015). Application of biochar for the removal of pollutants from aqueous solutions. *Chemosphere*, 125, 70–85. <https://doi.org/10.1016/j.chemosphere.2014.12.058>
- Tayibi S, Monlau F, Oukarroum A, Zeroual Y (2020) One-pot activation and pyrolysis of Moroccan Gelidium ses quipedale red macroalgae residue: production of an efficient adsorbent biochar. *Biochar* 1:401–412. <https://doi.org/10.1007/s42773-019-00033-2>
- Traoré M, Kaal J, Cortizas AM (2015) Application of FTIR spectroscopy to the characterization of archeological wood. *SAA* 153:63– 70. <https://doi.org/10.1016/j.saa.2015.07.108>
- Tsai, W. T., Kuo, L. A., Tsai, C. H., Huang, H. L., Yang, R. Y., & Tsai, J. H. (2023). Production of Porous Biochar from Cow Dung Using Microwave Process. *Materials*, 16(24), 7667. <https://doi.org/10.3390/ma16247667>
- Tsai, W. T., Lee, M. K., & Chang, Y. M. (2006). Fast pyrolysis of rice husk: Product yields and compositions. *Bioresource Technology*, 98(1), 22–28. <https://doi.org/10.1016/j.biortech.2005.01.016>
- Uday, V., Harikrishnan, P. S., Deoli, K., Zitouni, F., Mahlkecht, J., & Kumar, M. (2022). Current trends in production, morphology, and real-world environmental applications of biochar for the promotion of sustainability. *Bioresource Technology*, 359, 127467. <https://doi.org/10.1016/j.biortech.2022.127467>
- Wang, S., Su, D., Xu, W. (2022). Vegetation restoration with Dodonaea v. improves soil nutrients and aggregate stability in a degraded karst ecosystem. *Land*, 11(8), 1140. <https://doi.org/10.3390/land11081140>
- Wang Y, Ke L, Peng Y et al (2020a) Ex-situ catalytic fast pyrolysis of soapstock for aromatic oil over microwave-driven HZSM-5@SiC ceramic foam[J]. *Chem Eng J* 402, 126239. <https://doi.org/10.1016/j.cej.2020.126239>
- Widayat, W., Darmawan, T., Hadiyanto, H., Rosyid, R.Ar.(2017). Preparation of Heterogeneous CaO Catalysts for Biodiesel Production. *Journal of Physics Conference Series*, 877(1), 012018. <https://doi.org/10.1088/1742-6596/877/1/012018>
- Xie, C., Yuan, L., Tan, H., Zhang, Y., Zhao, M., & Jia, Y. (2021). Experimental study on the water purification performance of biochar-modified pervious concrete. *Construction and Building Materials*, 285, 122767. <https://doi.org/10.1016/j.conbuildmat.2021.122767>
- Xu, X., Guo, Y., Shi, R., Chen, H., Du, Y., Liu, B., ... & Li, L. (2021). Natural Honeycomb-like structure cork carbon with hierarchical Micro-Mesopores and N-containing functional groups for VOCs adsorption. *Applied surface science*, 565, 150550. <https://doi.org/10.1016/j.apsusc.2021.150550>
- Yahya, S. A., Iqbal, T., Omar, M. M., & Ahmad, M. (2021). Techno-economic analysis of fast pyrolysis of date palm waste for adoption in Saudi Arabia. *Energies*, 14(19), 6048. <https://doi.org/10.3390/en14196048>
- Yang, C., Shang, H., Li, J., Fan, X., Sun, J., & Duan, A. (2023). A review on the microwave-assisted pyrolysis of waste plastics. *Processes*, 11(5), 1487. <https://doi.org/10.3390/pr11051487>
- Zafeer, M. K., Menezes, R. A., Venkatachalam, H., & Bhat, K. S. (2024). Sugarcane bagasse-based biochar and its potential applications: a

- review. *Emergent Materials*, 7(1), 133-161. <https://doi.org/10.1007/s42247-023-00603-y>
- Zhang J, You C (2013) Water holding capacity and absorption properties of wood chars. *Energy Fuels*, 27,2643–2648. <https://doi.org/10.1021/ef4000769>
- Zhang, J., Liu, J., Liu, R., (2015a). Effects of pyrolysis temperature and heating time on biochar obtained from the pyrolysis of straw and lignosulfonate. *Bioresour. Technol.* 176, 288–291. <https://doi.org/10.1016/j.biortech.2014.11.011>
- Zhang, Y., Fan, S., Liu, T., Fu, W., & Li, B. (2022). A review of biochar prepared by microwave-assisted pyrolysis of organic wastes. *Sustainable Energy Technologies and Assessments*, 50, 101873. <https://doi.org/10.1016/j.seta.2021.101873>
- Zhou, Y., Qin, S., Verma, S., Sar, T., Sarsaiya, S., Ravindran, B., ... & Awasthi, M. K. (2021). Production and beneficial impact of biochar for environmental application: a comprehensive review. *Bioresour. Technology*, 337, 125451. <https://doi.org/10.1016/j.biortech.2021.125451>.
- Zhu, L., Lei, H., Wang, L., Yadavalli, G., Zhang, X., Wei, Y., ... & Ahring, B. (2015). Biochar of corn stover: Microwave-assisted pyrolysis condition induced changes in surface functional groups and characteristics. *Journal of Analytical and Applied Pyrolysis*, 115, 149-156. <https://doi.org/10.1016/j.jaap.2015.07.012>



© 2025. The Author(s). This article is an open access article distributed under the terms and conditions of the Creative Commons Attribution-ShareAlike 4.0 (CC BY-SA) International License (<http://creativecommons.org/licenses/by-sa/4.0/>)